

# Defect detection in photovoltaic modules using electroluminescence imaging

Amine Mansouri, Technische Universität München, Arcisstr. 21, 80333, Munich  
amine.mansouri@tum.de, +49 89 30785137

Marcus Zettl, Oliver Mayer, Mark Lynass, Martin Bucher, Omar Stern, Christian Heller, Eike Mueggenburg. GE Global Research, Freisinger Landstr. 50, 85748 Garching

## Subject: 4.1

### I. ABSTRACT

*Electroluminescence (EL) imaging for photovoltaic applications has been widely discussed in the last years. In this contribution, the results of an all-around evaluation of this technique in regard to defect detection and quality assessment in photovoltaic modules are presented. The aptitude of the EL system for detecting failures and deficiencies in both crystalline and thin film PV modules (CdTe and CIGS) is thoroughly analyzed and an exhaustive defect catalogue is established. In crystalline silicon devices, cell breakages resulting from micro-cracks were proven to represent the major problem and remarkably affect the module performance. A linear correlation between the size of the breakages and the power drop in the module could be established. Further, mechanical stress and temperature change could be identified as the major cause behind the proliferation of cracks and breakages. In thin film modules, EL imaging proved a remarkable reduction in the size of localized shunts under the effect of light soaking (together with a performance improvement of up to 8%). Aside from that, the system voltage was applied for monitoring TCO corrosion effects, laser scribing induced failures, as well as several problems related to the module junction box in regard to its sealing and the quality of its electric connectors.*

**Index Terms**—Electroluminescence (EL), PV defects, failure catalogue, cell breakages, micro-cracks, shunts, potential induced degradation (PID)

### II. INTRODUCTION

PHOTOVOLTAIC cells are optimized for absorbing light and converting it into electricity. Due to the reciprocity principle, they can also be stimulated to emit photons and offer therefore, the foundation of the optical characterization techniques. Over the last few years, a variety of optical tools, which partially had been developed for other applications, have been probed for quality assessment in the photovoltaic industry. Electro-Luminescence (EL), Photo-Luminescence (PL), Laser Beam Induced Current imaging (LBIC) and Thermal imaging are the most-known examples.

Electroluminescence (EL) is an optical phenomenon which has been used for a long time [1] in lightening

applications and recently integrated as an investigation procedure for photovoltaic devices. It consists in applying a direct current to the module and measuring the Photoemission by means of an infrared-sensitive camera. The brightness distribution on the photography correlates with the distribution of the open circuit voltage, the minority carrier diffusion length, the series resistance, as well as with the quantum efficiency and the ideality factor of the examined cell [2, 3, 4, and 5]. The work in hand focuses on presenting the measurement setup of EL-Imaging and evaluating its capacities regarding quality assessment and defect detection in solar cells and modules of different technologies.

### III. ELECTROLUMINESCENCE MEASUREMENT SYSTEM

#### A. Used equipment

In this work, a back-illuminated Si-CCD camera from Great Eyes with a high near infrared (NIR) sensitivity (quantum yield 85% @ 750nm, 40% @ 900nm and 10% @ 1000nm) was used. The system features an image size of 1024x1024 pixels and a pixel size of 13 $\mu$ m x 13 $\mu$ m. The dynamic range of the recorded data amounts to 16bit. The used camera is equipped with a Minolta MD W.Rokkor Objective with a focal length of 35mm and a maximum F-number of f/1.8. The system is mounted on a freely movable tripod inside an extra dimmed black tunnel, allowing for both close-up measurements of different module sections - with a minimum camera-object distance of 30cm- and overall shots of complete modules. The 5.5m tunnel length allows the measurement of all common panel sizes of up to 2m x 2m.

The power supply is ensured by a TDK-Lambda GEN100-15 programmable DC unit with a maximum voltage output of 100V and a maximum current output of 15A. The integrated synchronization module allows the control of the EL camera as well as the communication with the measurement software. For measuring thin film modules with particularly high open circuit voltages, a Delta Elektronika power supply providing up to 140V and 13A is used. The user-system interaction is assured by the LumiSolar Mobile software.

The system validation occurred through a qualitative and quantitative comparison of EL measurements of two reference modules by the system in hand and by an electroluminescence setup at the Fraunhofer ISE research center in Freiburg.

## B. System parameter optimization

### Aperture size and exposure time

In the used system, exposure times longer than 1s turned out to have minimal effect on the measured luminescence and the image quality. The well dimmed black tunnel lets little stray light through and an F-number of 2.8 (one closing level of the aperture) allows optimal results. Fig. 1 shows the mean value and the standard deviation of the gray values from 10 close-up images of a CdTe thin film module, taken with exposure times between 0.05s and 30s. Only images made in less than 1s feature a lower brightness and show less details.

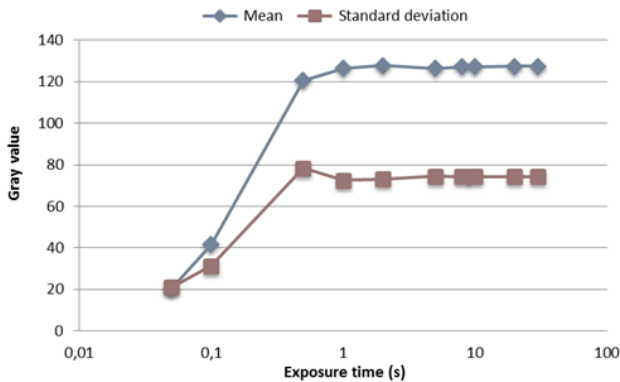


Fig. 1. Image brightness as a function of the exposure time

### Operating voltage and current

The purpose of applying an electric voltage during the electroluminescence imaging is to counter the depletion zone electric field and hence allow the charge carriers to diffuse into the junction and recombine. The diffusion process starts when the applied voltage reaches the  $V_{oc}$  level. Due to the internal resistance of the power supply, higher voltages are needed in order to achieve sufficient recombination rates and good quality results.

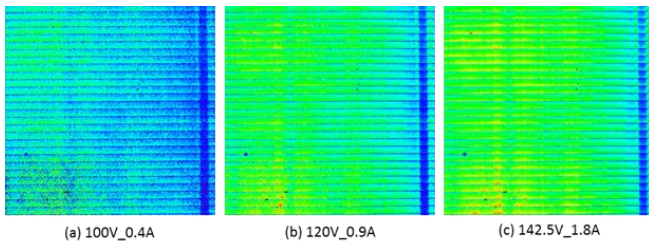


Fig. 2. Effect of operating voltage and current on image quality

Fig. 2 is an image sequence, taken at different voltage and current values, showing a section of a CdTe thin film module ( $V_{oc} = 92V$ ,  $I_{sc} = 1.2A$ ). Below 120V (a), the weak recombination is unable to provide sufficient luminescence and reveal all module details. Optimal results are achieved with a voltage 30% higher than  $V_{oc}$  (b). Images taken at very high voltages and current flows above  $I_{sc}$  (c) show inhomogeneous luminescence at the cell boundaries. This effect is due to the domination of the module series resistance. Furthermore, very high currents tend to accelerate the module heating and thus to distort the measured luminescence.

### Camera position and focal length

Fig. 3 shows the relation between image size, focal length and camera position based on 4 measurements of a CdTe thin film module. An almost linear correlation could be noticed. Focal length values between 1.5m and 3m, and camera positions between 30cm and 4.5m cover all image

sizes from 20cm x 20cm close-up views to 2m x 2m overall measurements of large-size modules. However, a fine-tuning of the camera focal length is needed almost always. The various materials, layer structures, module thicknesses etc. make the determination of a unique relation impossible.

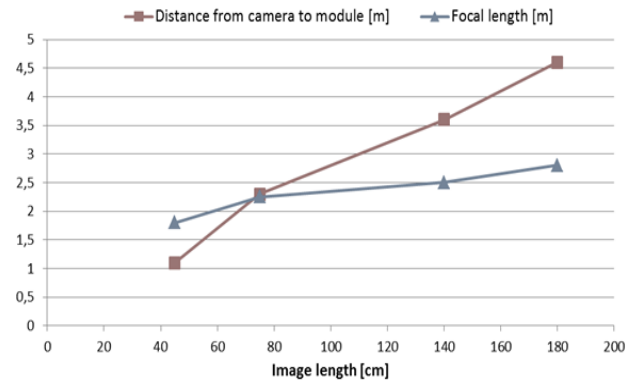


Fig. 3. Image size, camera position and focal length

## IV. DEFECTS OF CRYSTALLINE SILICON MODULES

### A. Cracks and breakages

Cracks and breakages in the semiconductor material are responsible for the majority of power loss cases in crystalline silicon cells. The cracks generally propagate parallel to the contact fingers of the module and thus impact only the cracked area (0.9A of current dissipation for a cm crack length [6]). In some cases, cracks can also propagate perpendicularly to the contact fingers and damage them resulting in the development of cell breakages. Fig. 4 shows the typical appearance of cell cracks and breakages in crystalline silicon PV.

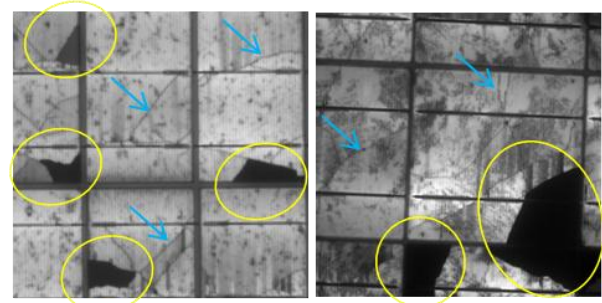


Fig. 4 Cracks and breakages in crystalline silicon cells

In order to accurately assess the effect of cell breakages on the device performance, the output power of 4 modules of different sizes were measured using the flash solar simulator. For each module, an electroluminescence measurement has been performed and the breakage areas, appearing dark in the EL image (Gray value less than 50) were integrated. A direct correlation between the total breakage area and the power drop could easily be noticed. The comparison results are shown in fig. 5.

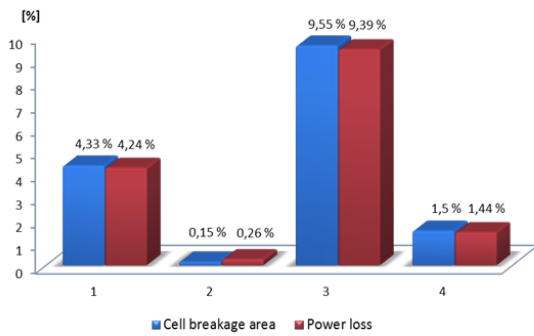
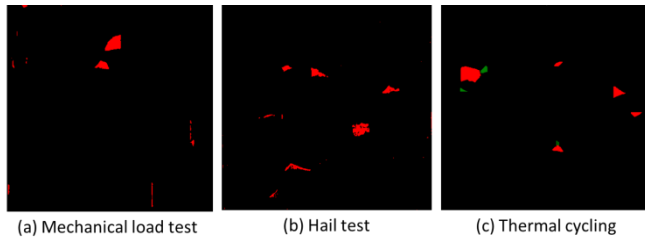


Fig. 5 Correlation between cell breakage area and power loss

In order to determine the reasons behind the occurrence and propagation of cell cracks and breakages, several crystalline silicon modules were exposed to different stress conditions and the EL measurements before and after the experiment were compared. The comparison occurred through the subtraction of the resulting image from the original image using the processing software ImageJ. All pixels featuring a gray value over 70 and corresponding to the newly formed cracks and breakages are marked in red. Fig. 6 presents the resulting images of the stress tests.



The application of a mechanical load of approximately 4500Pa for a duration of 2h on a polycrystalline silicon module (front and rear side) induced the occurrence of several new cracks as well as the development of a number of cell breakages, generally situated between two preexisting cracks (fig. 6a). Similar effects could be noticed under the influence of punctual, short-term strains such as the impact of hailstones (simulated using a hail cannon and average-size ice balls). The corresponding difference image is represented in fig. 6b. On the other hand, temperature cycling experiments showed no conclusive degradation effect: Several modules were exposed to 5 temperature cycles of 10 hours varying between  $-40^{\circ}\text{C}$  and  $+85^{\circ}\text{C}$  in the climate chamber. Some new cracks and breakages appeared (fig. 6c: red) and some defective areas appear to have regained their activity (fig. 6c: green). This effect can be explained by the expansion and contraction of the metallic contact fingers under the effect of changing temperature. Depending on their position and depth, contact interruptions due to cell cracks can be restored or extended.

### B. Crystal inhomogeneity

A further imperfection of crystalline silicon cells, which can easily be detected using EL imaging, is the crystal inhomogeneity, appearing in the EL image as distributed dark areas with granular aspect (fig. 7). These inhomogeneities can have various reasons [7]: process related fluctuations in dopant concentration or in material thickness, inherent inhomogeneities related to structural defects and to the quality of the material itself etc. The crystal inhomogeneities lead to inhomogeneous band gap widths and thus to a lower efficiency of the cell.



Fig. 7 Crystal inhomogeneities in crystalline silicon cells

### C. Defective edge isolation

During the edge isolation process, short circuits can occur. The voltage drop between the n-doped and the p-doped semiconductor of the p-n-junction decreases, leading to a weaker electroluminescence signal detectable in the measured data. Fig. 8 shows a section of a polycrystalline silicon module showing defective isolation on the cell edges.

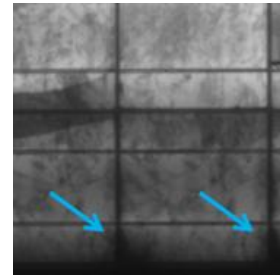


Fig. 8 Defective edge isolation

### D. Contact grid interruptions

Due to various problems during the module manufacturing and operation, the metallic fingers assuring the front contact can be locally interrupted. Depending on the position and width of the contact gap, the impact of this defect on the module power output can greatly vary. Contact finger interruptions situated on the cell edges pose a particular problem. In the utter fingers of the solar cell, the current is injected by a single bus bar. Therefore, the finger interruption induces a complete contact outage between the finger gap and the cell edge. In the electroluminescence image, these defects are easily detectable in the form of dark areas surrounding the interrupted finger and reaching to the cell edges (fig. 9).

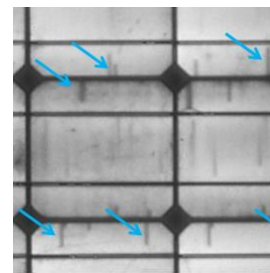


Fig. 9 Contact finger interruptions in a mono-crystalline silicon cell

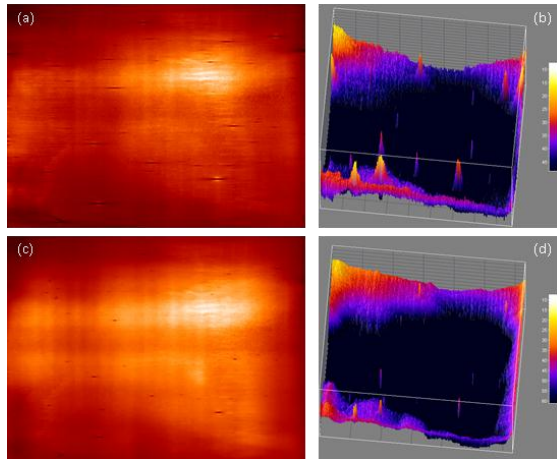
## V. DEFECTS OF THIN FILM MODULES

### A. Shunts

Shunts are localized leakage currents between the front and the rear contact of the solar cell. The low resistance of shunted spots induces a low open circuit voltage and thus a lower fill factor of the cell. Several mechanisms can be behind the occurrence of shunts: failures in the deposition procedure resulting in a discontinued or a locally too thin p-type semiconductor layer, faulty laser scribing inducing p-n junction damage, the presence of dust particles or metal

traces etc. Shunts have a very particular EL brightness pattern: a localized darkness within a single cell having a particularly dark center and a symmetric appearance along the cell. In some cases, the shunt center can feature a very high electroluminescence signal referring to a non-linear shunt caused by a recombination-active crystal defect or to a high thermal radiation signal induced by the great current density through the shunt [8]. In the scope of this work, shunts could rarely be noticed in crystalline modules and were very frequent in thin film devices, especially those based on CIGS.

Within the investigation of local shunts, it could be proven that light soaking treatment remarkably affects the size of the shunts and thus their impact on the module performance. Fig. 10 represents a CIGS module after a long-term dark storage (a and b) and after 24h in the light soaking station under  $1000 \frac{W}{m^2}$  (c and d). We notice a remarkable reduction in the size of the dark areas surrounding the shunted spots as well as an increase of the operating voltage (+6.3%) and the module output power (+8%). This observation could be explained by a light soaking induced rise of the charge carrier density and hence of the operating voltage as suggested in [9] and [10].



### B. TCO corrosion

The corrosion of the transparent conductive oxide layer is known to mainly affect modules based on glass substrates when exposed to high negative voltages at high temperatures and humidity levels [11, 12]. The corroded front contact interrupts the charge carrier transport into the junction and the affected areas appear dark in the EL image. Since the moisture penetration occurs at the module edges, the dark areas are concentrated in the outer zone of the module. In order to investigate the correlation between the TCO corrosion and the power drop in thin film panels, a CdTe based module was reverse-biased under 1kV for 250 hours in a controlled environment inside the climate chamber (85°C and 85% of relative humidity). Power and EL measurements were performed before, after and within the test (Fig. 11). A linear dependence between the corroded area (darkness in the EL image) and the power drop could be shown.

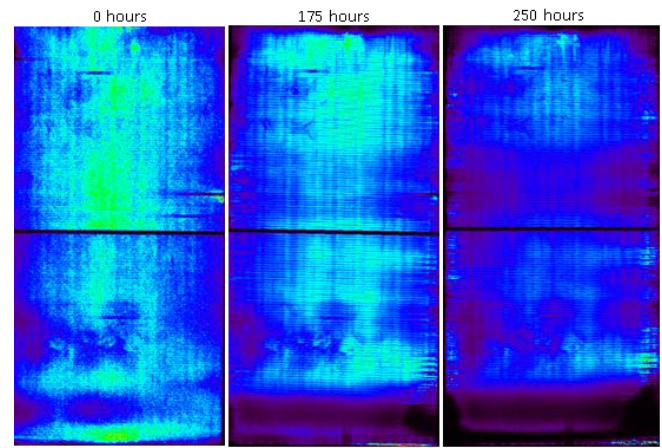


Fig. 11 Progression of the TCO corrosion in a thin film CdTe module

### C. Laser scribing failures

During the laser scribing process for cell isolation and module structuring, various failures can occur. First, the semiconductor layer can be erroneously skimmed inducing localized shunts on the cell edge. Besides, the cell interconnection (the metallic rear contact or the TCO front contact) can be damaged increasing the series resistance and impeding the current flow between the cells, which compromises the module performance. The damaged interconnections appear as dark areas surrounding the laser scribe lines and covering variously large parts of the adjacent cells. Fig. 12 illustrate this effect in 4 different CdTe modules and point out the effect of stress situations in accelerating the failure process.

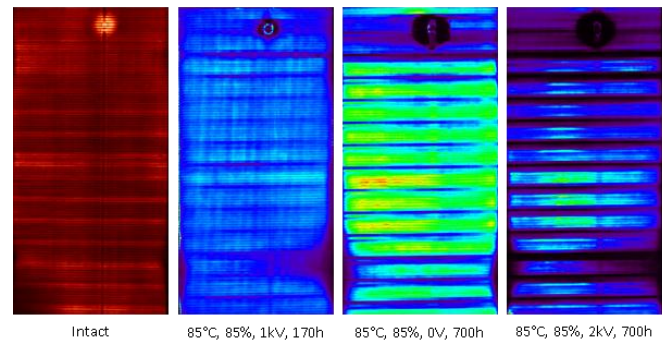


Fig. 12 Damaged cell interconnection due to defective scribing process

### D. Junction box failures

Electroluminescence imaging allows an accurate and quick assessment of the contact quality in the junction boxes of thin film modules. Unlike in thick crystalline cells, the thinness of the cell layers in thin film devices allows the detection of radiation signals emitted by the junction box. If the interconnection between the cell string and the solar cable features a high resistance due to defective soldering or bad quality materials, the current flow is hampered and the junction box heats up. The emitted thermal radiation can partially be detected by the electroluminescence camera and the surroundings of the box appear very bright on the EL image. The radial appearance of this high luminescence confirms the assumption of its thermal nature. If the junction box is not properly sealed, moisture can ingress and damage the module. In the area surrounding the junction box, the TCO is delaminated and no current can be injected into the cell. Therefore, no recombination occurs and the affected area appears dark in the EL measurement.

## VI. CONCLUSION

In this work, EL imaging was shown to represent a powerful quality assessment tool for both crystalline and thin film solar modules. When properly adjusted and configured, the system is able of accurately detecting numerous failures and ageing effects in very short times.

## REFERENCES

- [1] R.D. Dupuis, M.R. Krames, *History, Development, and Applications of High-Brightness Visible Light-Emitting Diodes*. Journal of Lightwave Technology, Vol. 26, No. 9, pp. 1154 – 1171. May 2008.
- [2] P. Würfel, T. Trupke, T. Puzzer, E. Schäffer, W. Warta, S. W. Glunz *Diffusion lengths of silicon solar cells from luminescence images*. J. Appl. Phys. 101, 123110. 2007
- [3] T. Fuyuki, Y. Kaji, A. Ogane, Y. Takahashi. *Analytic findings in the photographic characterization of crystalline silicon solar cells using electroluminescence*. IEEE 4th world conference on photovoltaic energy conversion. 2006
- [4] M. Köntges, M. Siebert, D. Hinken, U. Eitner, K. Bothe, T. Potthof. *Quantitative analysis of PV-modules by electroluminescence images for quality control*. 24th European Photovoltaic Solar Energy Conference, Hamburg, Germany, 21-24 September 2009, 4CO.2.3
- [5] D. Hinken, K. Ramspeck, K. Bothe, B. Fischer, R. Brendel. *Series resistance imaging of solar cells by voltage dependent electroluminescence*. Appl. Phys. Lett. 91, 182104. 2007
- [6] C. G. Zimmermann. *Utilizing lateral current spreading in multijunction solar cells: An alternative approach to detecting mechanical defects*. J. Appl. Phys. 100, 023714. 2006
- [7] J. Salinger, V. Benda, F. Z. Machacek. *Optimal Resolution of LBIV/LBIC Methods for Diagnostics of Solar Cell Homogeneity*. Proc. 26th International Conference on Microelectronics, Niš, Serbia. May 2008.
- [8] T. Weber, E. Benfares, S. Krauter, P. Grunow. *Electroluminescence on the TCO corrosion of thin film modules*. 25th European Photovoltaic Solar Energy Conference and Exhibition / 5th World Conference on Photovoltaic Energy Conversion, Valencia, Spain. Sep. 2010
- [9] M. Igalson, M. Cwil, M. Edoff. *Metastabilities in the electrical characteristics of CIGS devices: Experimental results vs. theoretical predictions*. Thin Solid Films, vol. 515, pp. 6142-6146. 2007.
- [10] F.-J. Haug, D. Rudmann, H. Zogg, A.N. Tiwari. *Light soaking effects in Cu(In,Ga)Se<sub>2</sub> superstrate solar cells*. Thin Solid Films 431 –432. 2003.
- [11] D. E. Carlson, R. Romero, F. Willing, D. Meakin, L. Gonzalez, R. Murphy, H. R. Moutinho, M. Al-Jassim. *Corrosion Effects in Thin-Film Photovoltaic Modules*. Prog. Photovolt: Res. Appl. 11:377–386. 2003.
- [12] K. W. Jansen, A. E. Delahoy. *A laboratory technique for the evaluation of electrochemical transparent conductive oxide delamination from glass substrates*. Thin Solid Films 423, 153–160. 2003.